

Enhancement of the irreversible axial-strain limit of Y-Ba-Cu-O-coated conductors with the addition of a Cu layer

N. Cheggour and J. W. Ekin

National Institute of Standards and Technology, Boulder, Colorado 80305

Y.-Y. Xie and V. Selvamanickam

SuperPower Incorporated, Schenectady, New York 12304

C. L. H. Thieme and D. T. Verebelyi

American Superconductor Corporation, Westborough, Massachusetts 01581

(Received 18 August 2005; accepted 30 September 2005; published online 18 November 2005)

A Cu protection layer added to yttrium-barium-copper-oxide-(YBCO-) coated conductors substantially enhances the irreversible strain limit ϵ_{irr} for the onset of permanent electrical damage of the composite. This enhancement is of significance since it enables these conductors to meet the most severe strain requirements for applications such as electric generators. The conductors studied had either a Hastalloy-C substrate with an ion-beam-assisted deposition template or a rolling-assisted biaxially textured Ni-W substrate. The irreversible strain limit, obtained from critical-current measurements as a function of axial tensile strain at 76 K and self-field, increased from about 0.4% to more than 0.5% for both types of coated conductors with an added Cu layer, either by electroplating or lamination. This improvement is due only partially to the differential thermal contraction between Cu and the other conductor components. We believe that the Cu layer also enhances the fracture toughness of YBCO, thus acting as crack inhibitor/arrester. © 2005 American Institute of Physics. [DOI: 10.1063/1.2136231]

Recent progress in the development of yttrium-barium-copper-oxide-(YBCO-) coated conductors has yielded significant improvement of the composite critical-current density J_c (in excess of 2 MA/cm²) and length (100 m).¹⁻⁵ Furthermore, a Cu layer is now readily added to the architecture of these conductors to improve their electric and thermal stability, beneficial for protecting the conductor during possible thermal runaway events, especially in applications at low cryogenic temperatures where current densities can be particularly high.

The conductor tolerance to axial strain ϵ now required for some applications, such as particular designs of superconducting generators, may reach 0.4% strain to accommodate stresses on the strands due to rotational forces in the device.⁶ Moreover, a higher tolerance of strands to strain will likely allow a reduction in the size of the mechanical-support structure of the generator coils, and hence a lower manufacturing cost of these devices.⁶ However, the best axial-strain performance of YBCO-coated conductors reported until now was a strain of about 0.4%,⁷ barely matching the stringent strain benchmark, without any safety margin.

In this Letter, we show that the incorporation of a Cu layer onto the structure of YBCO-coated conductors not only provides protection of the strand, but also enhances the tolerance of the conductor to axial strain substantially beyond the prescribed strain benchmark. Of significance, this valuable improvement is obtained with two different coated-conductor fabrication techniques: ion-beam assisted deposition (IBAD) templates on Hastalloy-C substrates^{5,8} and rolling-assisted biaxially textured Ni-W substrates (RABiTS).^{3,9} The Cu layer is added by either electroplating or lamination.

The irreversible strain limit ϵ_{irr} , representing the strain at the onset of YBCO cracking,⁷ increases from about 0.4% to

more than 0.5%. We demonstrate that the mismatch in thermal contraction between Cu and the other conductor components explains only part of the improvement of ϵ_{irr} . Other mechanisms play a role in order to account for the full magnitude of the enhancement of ϵ_{irr} .

The first group of samples investigated (designated by the prefix "A" in Table I) was obtained by the use of a metal-organic chemical vapor deposition (MOCVD) for growing YBCO on polished Hastalloy C-276 substrates with an IBAD template,^{5,8} followed by deposition of a thin Ag film on YBCO. The Cu layer was then electroplated over the structure. Cu was deposited either only on the YBCO side (samples A-Cu-1 and A-Cu-2) or on all sides, such that the conductor was fully encapsulated with Cu (samples A-Cu-3 and A-Cu-4). In both cases, the total thickness of Cu was similar, about 30 μm .

The second group of samples (designated by the prefix "B" in Table I) had YBCO grown on buffered Ni-5at.%W RABiTS by the use of a metal-organic deposition (MOD).^{3,9} A thin Ag layer was then deposited on YBCO and the conductor laminated by soldering a Cu foil onto it on the YBCO side. The thickness of the Cu layer (75 μm) matched that of the substrate, such that YBCO was located near the neutral axis of the conductor.

Most IBAD and RABiTS samples were slit to a width of 3 to 4 mm and pieces 3.5 cm long were used for the measurements. The variations in J_c , by a factor of about 2 within each group (Table I), are due solely to the fact that these samples were fabricated at different times during a period of 2 years, with the higher- J_c samples having been fabricated more recently. The increase in J_c shows the remarkable progress made in the development of the YBCO-coated conductors and does not otherwise affect any of the conclusions of this work.

TABLE I. Physical and electromechanical properties of YBCO-coated conductors fabricated by using either Hastalloy-C substrates with an IBAD template or Ni-W RABiTS substrates. Measurements were performed at 76 K. Values of J_c and I_c were determined at a $1 \mu\text{V}/\text{cm}$ criterion.

Sample no.	Fabrication process	Substrate; t_S^a (μm)	t_{YBCO}^a (μm)	t_{Ag}^a (μm)	t_{Cu}^a (μm)	Process of Cu addition	Initial J_c (MA/cm^2)	Initial I_c (A/cm width)	Initial n value ^b	$\varepsilon_{\text{irr}}^c$ (%)
A1	IBAD/MOCVD	Hastalloy C-276; 100	1.1	3	0	N/A	0.95	105	30	0.43
A2	"	"	1.1	3	0	"	1.60	176	40	0.40
A3	"	"	1	7	0	"	2.17	217	43	0.41
A-Cu-1	"	"	1	3	30	Cu plating; YBCO side	2.13	213	41	0.54
A-Cu-2	"	"	1	3	30	"	2.24	224	47	0.53
A-Cu-3	"	"	1.2	3	30	Cu plating; all sides	2.07	248	33	0.48
A-Cu-4	"	"	1.2	3	30	"	1.86	223	28	0.48
B1	RABiTS/MOD	Ni-5at.%W; 75	1	14	0	N/A	1.03	104	39	0.38
B2	"	"	1	3	0	"	0.87	87	30	0.38
B-Cu-1	"	"	0.8	3	75	Cu lamination; YBCO side	1.62	130	39	0.50
B-Cu-2	"	"	0.8	3	75	"	1.61	129	36	0.50
B-Cu-3	"	"	0.8	3	75	"	2.09	167	35	0.56

^a $t_S, t_{\text{YBCO}}, t_{\text{Ag}}, t_{\text{Cu}}$: thicknesses of substrate, YBCO, Ag, and Cu layers, respectively.

^b n value: exponent in the fit $V \propto I^n$ of the V - I curves around the critical current I_c .

^c ε_{irr} : strain limit at which any $I_c(\varepsilon)$ degradation becomes irreversible.

The measurements of J_c vs ε were made in liquid nitrogen at about 76 K, in the self-field, by the use of a test apparatus that permits stress-free cooling of the sample. The critical current I_c was determined from the voltage versus. current (V - I) curves with an electric-field criterion of $1 \mu\text{V}/\text{cm}$, and J_c was calculated from the cross-sectional area of YBCO. Uncertainties in I_c and the YBCO cross section were, respectively, about 1% and 10%. Strain was determined with a calibrated extensometer placed directly at the sample location. All strain data were expressed in terms of *applied* axial strain. Uncertainty in the measurement of strain was about $\pm 0.02\%$.

Typical $J_c(\varepsilon)$ curves are depicted in Figs. 1 and 2 respec-

tively for IBAD and RABiTS conductors; an overall view of the data is summarized in Table I. The procedure for data acquisition consisted of incrementally increasing the applied strain and measuring its corresponding value of J_c . The sample was periodically unloaded to nearly zero stress, and J_c was measured for each unloaded point (primed points in Figs. 1 and 2). This allows the determination of the critical strain for which the corresponding unloaded point no longer retraces the J_c vs ε curve reversibly—a direct consequence of crack initiation in the YBCO layer.⁷ This irreversible strain limit ε_{irr} is probably the most relevant strain parameter, compared with other strain limits defined at arbitrary J_c -degradation criteria.⁷

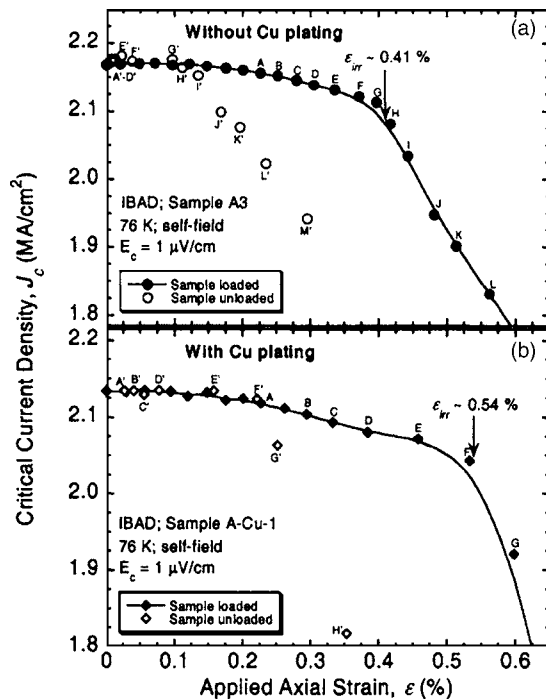


FIG. 1. A comparison of $J_c(\varepsilon)$ at 76 K and the self-field for YBCO films on Hastalloy C-276 substrates with an IBAD template, with and without a Cu-plated layer. The irreversible strain limit ε_{irr} improved substantially for the Cu-plated IBAD-coated conductors.

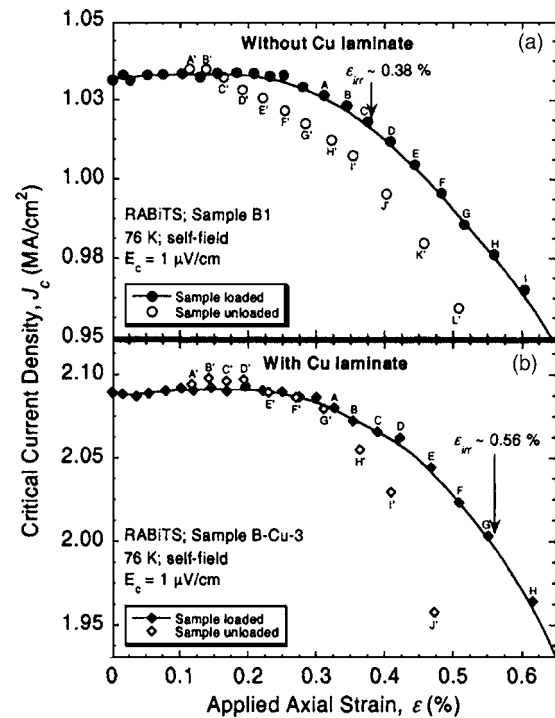


FIG. 2. A comparison of $J_c(\varepsilon)$ at 76 K and the self-field for YBCO films on Ni-5at.%W RABiTS, with and without a Cu-laminated layer. The irreversible strain limit ε_{irr} improved substantially for the Cu-laminated RABiTS-coated conductors.

Figure 1 shows an increase of ε_{irr} from 0.41% for sample A3 with no Cu to 0.54% for sample A-Cu-1, which has a 30 μm -thick Cu-plated layer on the YBCO side of the conductor. The average improvement of ε_{irr} for this type of sample is $\approx 0.12\%$ strain. The enhancement of ε_{irr} for IBAD samples with a surround layer of Cu of the same total thickness (15 μm on each side; samples A-Cu-3 and A-Cu-4) is only $\approx 0.07\%$ strain (Table I). Figure 2 shows very similar behavior for RABiTS conductors. For these composites, ε_{irr} increases on average by 0.14% strain when laminated with a Cu foil 75 μm thick on the YBCO side of the conductor. Therefore, for both IBAD and RABiTS conductors, adding a Cu layer enhances ε_{irr} enough that the coated conductors are able to meet the most severe strain requirements for applications.

Considering that Cu has a higher thermal contraction compared to both Hastalloy-C and Ni-W substrates when cooled to 76 K from room temperature or lamination temperature (~ 470 K),¹⁰ the YBCO layer would be under an additional pre-compression when Cu is added to the conductor structure. Due to the differential thermal contraction, each element of the composite will be subjected to an internal force. At equilibrium, the sum of all these forces is zero. The strain on the component i of the conductor after cooling to 76 K is

$$\varepsilon_i = \left(\frac{\Delta L}{L} \right)_i - \left(\frac{\Delta L}{L} \right)_{\text{comp}}, \quad (1)$$

where $(\Delta L/L)_i$ is the thermal contraction of component i on its own and $(\Delta L/L)_{\text{comp}}$ is the thermal contraction of the whole composite. Given that internal forces on components cancel each other, and assuming that none of the ductile materials yields in compression during cooling, $(\Delta L/L)_{\text{comp}}$ can be expressed as

$$\left(\frac{\Delta L}{L} \right)_{\text{comp}} = \frac{\sum_i S_i E_i \left(\frac{\Delta L}{L} \right)_i}{\sum_i S_i E_i}, \quad (2)$$

where S_i is the cross-sectional area and E_i is the modulus of elasticity of component i . Using the values of $(\Delta L/L)_i$ and E_i of each of the materials in the coated conductors¹⁰ and the respective thicknesses of these components (Table I), we can calculate the additional precompression of the YBCO layer from Eqs. (1) and (2). By electroplating Cu at room temperature and cooling the sample to 76 K, the YBCO layer in the IBAD conductors investigated will be under an additional compressive strain of only $\approx -0.016\%$, far below the 0.07% to 0.12% increase in ε_{irr} observed. In the case of the RABiTS conductors to which Cu was laminated at ≈ 470 K, the cooling of the sample from this temperature to 76 K subjects the YBCO layer to an additional compressive strain of $\approx -0.086\%$, only slightly more than half the average increase of ε_{irr} measured for this type of conductors ($\approx 0.14\%$). Hence, the differential thermal contraction, although it enhances ε_{irr} , does not account for the total increase of ε_{irr} .

The difference in the improvement of ε_{irr} between IBAD samples having Cu only on the YBCO side and those having the same total amount of Cu, but on all sides (i.e., half as much thickness on the YBCO side), is further evidence that the differential thermal contraction is not the only mechanism for the enhancement of ε_{irr} . This indicates that the thickness of Cu directly on the YBCO side may also be a relevant parameter in this process. It is known that the addition of metallic layers to ceramics greatly improves the fracture toughness of these brittle phases.¹¹ The added ductile phase shields (as a ligament) crack initiation zones behind the crack tips, thus acting as a crack inhibitor/arrestor. This process is more efficient when high yield-strength metals are used and also improves with the thickness of the metal layer.¹¹ We believe that a similar mechanism operates in YBCO-coated conductors. That is, the Cu layer enhances the fracture toughness of the YBCO film and, consequently, increases ε_{irr} . The Ag layer on YBCO may also serve somewhat as a crack arrestor, but the Cu layer is thicker and is probably more efficient than Ag alone due its higher yield strength. The metal substrate should also shield crack initiation sites located at the substrate/buffer interface. The increase in fracture toughness seems to be best achieved when the YBCO/buffer brittle layers are sandwiched between two appropriate ductile components (the substrate and protection layers).

Further optimization of ε_{irr} may still be possible by patterning the YBCO layer into strips before depositing Ag/Cu such that the ductile phase totally surrounds *narrow* YBCO subelements. We anticipate that crack arresting in this geometry would be even more efficient. It is also possible that the addition of a structural metal with mechanical properties superior to those of Cu would further increase ε_{irr} .

This work was supported by the U.S. Department of Energy, Office of Energy Delivery and Energy Reliability, and the Office of High Energy Physics.

¹P. J. Pellegrino, presentation at the DOE Wire Development Workshop, St. Petersburg, Florida, January 2005.

²A. Usoskin and H. C. Freyhardt, MRS Bull. **29**, 583 (2004).

³M. W. Rupich, D. T. Verebelyi, W. Zhang, T. Kodenkandath, and X. Li, MRS Bull. **29**, 572 (2004).

⁴Y. Iijima, K. Kakimoto, Y. Yamada, T. Izumi, T. Saitoh, and Y. Shiohara, MRS Bull. **29**, 564 (2004).

⁵V. Selvamanickam, Y. Xie, J. Reeves, and Y. Chen, MRS Bull. **29**, 579 (2004).

⁶J. Fogarty, presentation at the DOE Annual Peer Review, Washington DC, July 2004.

⁷N. Cheggour, J. W. Ekin, C. C. Clickner, D. T. Verebelyi, C. L. H. Thieme, R. Feenstra, and A. Goyal, Appl. Phys. Lett. **83**, 4223 (2003).

⁸V. Selvamanickam, G. Carota, M. Funk, N. Vo, P. Haldar, U. Balachandran, M. Chudzik, P. Arendt, J. R. Groves, R. DePaula, and B. Newnam, IEEE Trans. Appl. Supercond. **11**, 3379 (2001).

⁹D. T. Verebelyi, U. Schoop, C. Thieme, X. Li, W. Zhang, T. Kodenkandath, A. P. Malozemoff, N. Nguyen, E. Siegal, D. Buczek, J. Lynch, J. Scudiere, M. Rupich, A. Goyal, E. D. Specht, P. Martin, and M. Paranthaman, Supercond. Sci. Technol. **16**, 19 (2003).

¹⁰J. W. Ekin, *Experimental Techniques for Low Temperature Measurements* (Oxford University Press, UK, in press).

¹¹K. L. Hwu and B. Derby, Acta Mater. **47**, 545 (1999).